Production of BioSNG from waste derived syngas: pilot plant operation and preliminary assessment

M. MATERAZZI*, **, R. TAYLOR**, P. COZENS° AND C. MANSON-WHITTON°

** University College London, Department of Chemical Engineering – Torrington Place, London WC1E 7JE, UK*
*** Advanced Plasma Power Ltd, South Marston Business Park, Swindon SN3 4DE, UK*
° Progressive Energy Ltd, Swan House, Bonds Mill, Stonehouse, GL10 3RF, UK

Abstract:

Bio-substitute natural gas (or BioSNG) produced from gasification of waste fuels and subsequent methanation of the product gas could play a crucial role in the decarbonisation of heating and transportation, and could be a vital part of the energy mix in the coming decades. The BioSNG demonstration plant described in this paper seeks to prove the technical feasibility of the thermal gasification of waste to renewable gas, through a preliminary experimental programme to take an existing stream of syngas, methanate it and show that it can be upgraded to gas grid quality requirements. The syngas used in the project is a waste-derived syngas from a two-stage fluidised bed - plasma pilot facility, which is then converted and upgraded in a new, dedicated conversion and clean up plant. Extensive trials were undertaken on methanation and gas upgrading units for over 60 hours of continuous operation. The fundamentals of a once-through methanation process train have been established on the demonstration facility and a model built to extend the analysis over different operational parameters. Over the trials, methane outputs of greater than 50kW_{th}

output were routinely produced from three methanation reactors in series, with a total CO conversion exceeding 90% at pressures as low as atmospheric, in line with kinetic model predictions. Retention of CO_2 as well as adequate partial pressure of H_2O in the process stream was important for process control. The plant provided demonstration of the efficacy of a PSA system for separation of CO_2 (99% removal efficiency) as well as the potential to remove a proportion of residual H_2, N_2 and CO, although this was associated with appreciable CH_4 slip. The process can be optimized primarily by reducing inlet temperature to methanation reactors, controlling syngas composition and using adequate steam to carbon ratio, depending on the type of waste. This information can be used to inform the design and economics of subsequent planned commercial plants that could significantly increase the potential of renewable gas in the UK and elsewhere in Europe, providing a low cost route to low carbon heat and transport.

Keywords: BioSNG; Waste gasification; Methanation; Pilot plant

1. INTRODUCTION

Methane is an attractive heat and transport fuel vector. It is a clean and relatively low carbon intensity fuel, which can be utilised efficiently in the well-established infrastructure and demand-side technologies, such as gas boilers for heating and an increasingly wide range of gas vehicles (Uusitalo et al. 2014). Bio-methane produced from biomass or waste materials retains all the attributes of natural gas, with the crucial advantage that the fuel is renewable, offering substantial CO_2 emission savings. Biomethane is historically being produced via the upgrading of biogas from Anaerobic Digestion(Ardolino et al. 2018; Mao et al. 2015; Mata-Alvarez et al. 2000). However, in order to achieve a step change in production capacity,

alternative approaches such as via thermo-chemical routes (termed bio-substitute natural gas, or BioSNG) are necessary (Li et al. 2015; Seadi et al. 2008). Whilst technically feasible, this approach is less mature than anaerobic digestion. Transition from aspiration, to widespread operating facilities and infrastructure requires a detailed understanding of the technical and commercial attributes of the full chain, from feedstock supply through to delivery of grid quality gas, as well as the development of the first crucial operating facility which provides the tangible proof of concept for roll out (Cozens & Manson-Whitton 2010; E4tech 2014).

The demand for low carbon solutions for heat and transport through BioSNG is receiving increased international attention, especially in Europe with Gobigas project in Gothenburg and the Engie BioSNG research facility in Lyon (Arvidsson et al. 2012; Li et al. 2015; Rönsch et al. 2016). Both these facilities are focused on pure biomass feedstocks.

In light of the dominance of waste in the Europe bioenergy landscape as well as the wider economic and environmental attributes, the focus is rapidly shifting to waste-derived biomass. The production of Solid Recovered Fuel (SRF) or Refuse Derived Fuel (RDF) from non-hazardous wastes creates the opportunity to utilise wastes in thermal applications that are more sophisticated than the classical waste disposal route via incineration; in particular RDF, which contains up to 60-70% fraction (energy basis) of biomass (Iacovidou et al. 2018), is being regarded increasingly by a number of producers and users as a potential feedstock in gasification (Caputo & Pelagagge 2002). Hence, there is the potential for the transformation of combustible wastes into syngas and its products – including BioSNG, notwithstanding that new technical challenges associated to the heterogeneous composition of the waste materials are inevitably introduced. Whilst the production of substitute natural gas

from coal is a well-established process, being practiced for example at the Dakota synfuels plant for over 30 years (Kopyscinski et al. 2010; Li et al. 2014), production of BioSNG presents a number of issues demanding specific design choices and technical solutions. BioSNG plants must be at significantly smaller operational scale than coal to SNG plants (10-100MWth output compared with 1000MWth) due to the distributed nature of biomass and waste arising and lower energy density of the feedstock (Kopyscinski et al. 2010; Rönsch & Kaltschmitt 2012). This has important implications for many aspects of the plant design, specifically the gas processing and methanation approach. The chemistry and form of the feedstock, as well as scale of operation, means that unlike coal, it cannot be processed using established high intensity, high pressure entrained flow gasification (Gassner & Maréchal 2012). The available gasification technologies for this service tend to produce a syngas that contains a range of complex hydrocarbons ('tars') and other organic and inorganic contaminants (e.g. olefins, thiophenes, chlorides, etc.), whose presence and detrimental effects are not always appreciated (Kaufman-Rechulski et al. 2011). For example, at the modest commercial scale associated with waste fuelled facilities it would be economically impractical to use conventional energy intensive syngas scrubbing techniques (e.g. Rectisol or Selexol) to handle the entire range of sulphur contaminants found in the syngas (Rönsch & Kaltschmitt 2012).

The approach taken in this work is the use of a prepared syngas produced from a primary fluidised bed gasification unit, ideally suited to the conversion of heterogeneous feedstock with low melting point components (Arena & Di Gregorio 2014; Arena et al. 2015), and a second, high temperature syngas treatment stage, comprising an electric arc plasma converter (Materazzi et al. 2014). The advantage of splitting the waste conversion process in two separate stages, is that the

combined process is reasonably agnostic to changes in fuel composition, and can easily cope with the high ash loading produced by RDF gasification, which can be recovered as an environmentally stable, vitrified product from the second stage (Materazzi et al. 2015a). Furthermore, the high temperature in the second stage breaks down tars and sulphur bearing species such as thiophenes, delivering a carbon monoxide and hydrogen-rich intermediary gas which can be treated by conventional and readily scalable dry or wet gas processing/polishing techniques to remove contaminant components to the parts per billion levels required for methanation catalysis (Materazzi et al. 2015b). Indirect (or allothermal) gasification, an alternative approach taken in other BioSNG processes which physically separates char combustion from biomass steam (or CO_2) gasification, offers the potential efficiency advantages of a syngas containing up to 15% methane, as well as low inherent nitrogen levels without the need of an air separation unit (van der Meijden et al. 2010). However, this high methane content in this pyrolysis gas represents the gaseous end of a spectrum of complex and condensable hydrocarbons, including cyclic, polycyclic and sulphur containing organic species. Removal of large quantities of complex organics down to levels which can be tolerated by a catalyst is particularly challenging (Heidenreich & Foscolo 2015).

The design approach described in this paper is to produce syngas inherently free of any hydrocarbon, and rely on catalytic stages to selectively recombine atoms to the desired product. Furthermore, it is well known that methanation reaction rates can generate very high heat fluxes, which can lead to thermal degradation, localized coking and catalyst sintering (Bartholomew 1982). In coal-scale SNG facilities this is typically addressed by complex reactor design and recycling of product gas to minimise reactant concentration and remove reaction heat (Rönsch & Kaltschmitt

2012). In light of the scale of waste facilities, the strategic approach here is for a simplified once-through reactor system with the retention of carbon dioxide and use of steam as diluents to provide thermal buffering and moderation of the reactions.

In this paper, the thermodynamics and kinetics of the involved reactions are analysed through operation of a pilot plant with real syngas derived from wastes. This information would be key to properly design and optimize such reactors and, more importantly, to limit the risks during up-scaling from laboratory over pilot to commercial scale. For this purpose, a model is also developed in Aspen Plus to evaluate any differences in operating conditions, and to some extent, how different parameters affect the BioSNG efficiency of the systems. The systems will comprise water-gas shift reactor, methanation reactors, heat recovery, and product separation.

2. EXPERIMENTAL

2.1 Feedstock and Materials

The approach used in the BioSNG technology is inherently flexible in terms of feedstocks; the two-stage gasification system has demonstrated operation on a large range of feedstocks and, because of a separate shift reaction stage which provides means for H_2:CO ratio adjustment, the downstream methanation process is able to cope with a wide variety of syngas compositions from the gasifier. The experimental programme presented in this work has focused on waste feedstocks, primarily municipal solid waste (MSW), as this represents the most technically challenging feedstock with the highest treatment costs, and will be the focus of early plants in the future. Feedstocks such as waste wood would require minimal process adjustments.

This section provides the specification for the baseline feedstock utilised in experiments. The design point for the waste composition for the pilot facility is

derived from a number of datasets for representative residual municipal, commercial and trade waste collected nationally as well as locally. The design point specification is as shown in Table 1.

Table 1 Design point waste composition from local suppliers (Swindon, UK)

Category	Design Point	Lower limit	Upper limit
Paper (wt%)	30.36	19.47	64.00
Plastic Film (wt%)	5.72	3.55	17.80
Dense Plastics (wt%)	8.38	5.50	16.20
Textiles (wt%)	3.64	0.20	8.17
Disposable Nappies (wt%)	4.91	0.00	8.00
Misc Combustible (wt%)	6.40	2.29	10.92
Misc Non-Combustible (wt%)	6.08	0.00	8.93
Glass (wt%)	7.01	0.60	11.00
Putrescible (wt%)	16.82	3.00	27.00
Ferrous (wt%)	6.61	1.10	11.69
Non-ferrous (wt%)	1.96	0.60	2.90
Fines (wt%)	2.13	1.00	5.50
Total	100.00		
CV (MJ/kg)	10.05	9.08	13.62
RDF biomass content (wt%)	67.7	49.1	80.1
RDF biomass content (energy%)	64.1	39.9	79.8

Mass balance figures assume such waste is input to the facility in the form of wet RDF (i.e. shredded municipal waste with metals, glass, incombustibles and large objects removed), which is then dried on-site; the data presented on Table 2 gives an indicative specification for the RDF, based on the waste described above.. As all emerging technologies, implementation of BioSNG from MSW can only take place at this time with the appropriate tax, incentive and legislative environment. For example, the Renewable Obligation (RO) is the most established instrument in the UK to incentivise the use of biogenic resource (in this specific definition for provision of electricity only) (Ofgem 2016). A key parameter for understanding the renewable attributes of the BioSNG produced is, therefore, the biomass content of the

feedstock; the biomass content of RDF consists of its biodegradable fraction and is usually represented by the percentage of biogenic carbon (C-14) in comparison to the total carbon present in RDF, or as renewable energy fraction of the total calorific value of the feedstock (which also includes fossil derived components, like plastics). The default assumption used for the Renewables Obligation Order is a biomass content of at least 50% (on energy basis) (Ofgem 2016), which is in line with the figure of ~60% biomass content measured in this case.

Table 2 Baseline feedstock specification used for tests

	RDF (as received)
Description:	
Proximate analysis, % (w/w)	
Fixed carbon	6.4
Volatile matter	59.6
Ash	19.1
Moisture	14.9
Ultimate analysis, % (w/w)	
C	41.0
H	5.7
O	17.5
N	1.2
S	0.2
Cl	0.4
GCV, MJ/kg (dry basis)	22.1
Avg. biomass fraction (% GCV)	64.1

2.2 Test Facility

The syngas used in the project is a waste-derived syngas from Advanced Plasma Power's (APP) existing gasification pilot facility, located at Swindon (UK), which is converted and refined in a new, dedicated conversion and conditioning plant (Materazzi et al. 2017). These are shown in the process flow diagram below. A full description of the two parts of the plant is provided in this section.

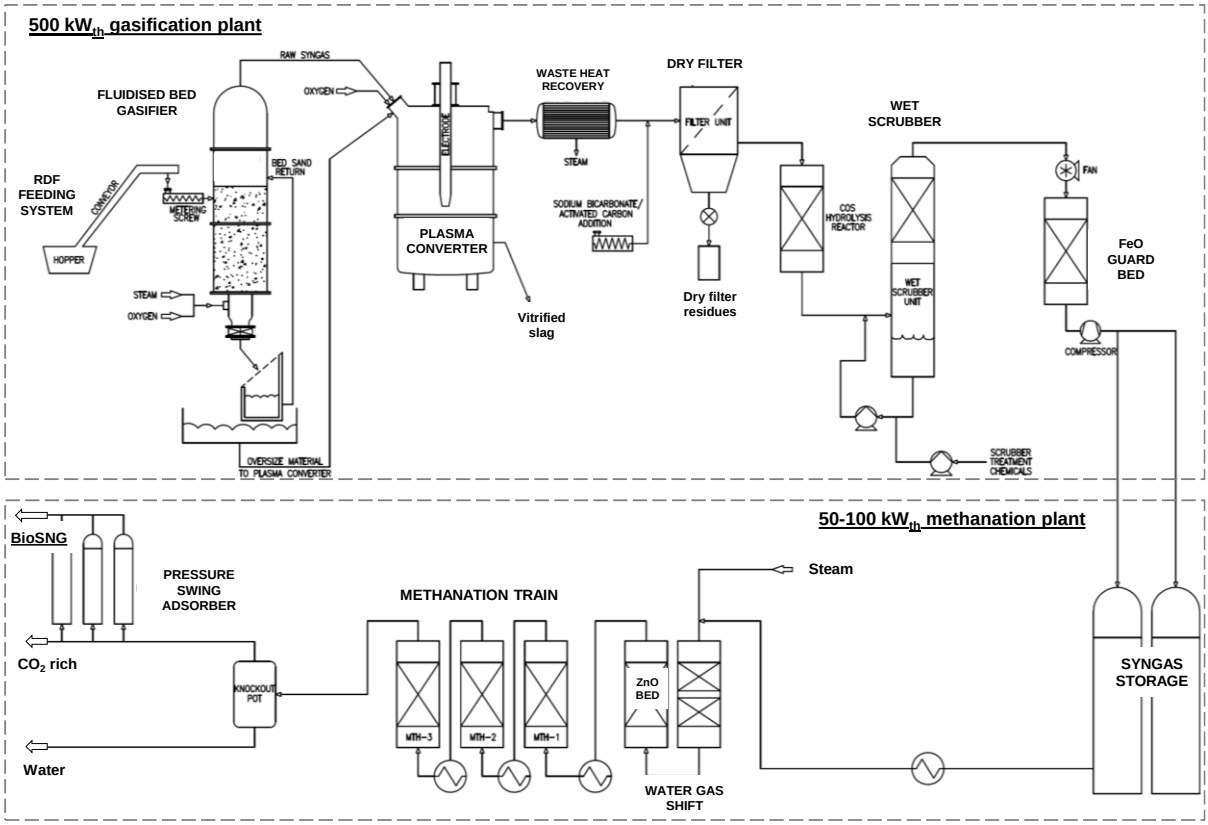

Figure 1: Integrated BioSNG pilot plant schematic. Top part relates to the previously exisisting 500 kWth plant for clean syngas production from RDF (Materazzi et al. 2016). Produced syngas is compressed and stored at 60 barg in storage vessels (bottom), before being directed to the new (50-100 kWth) chemical and gas separation sections.

2.2.1. The two-stage gasification process

The gasification process is a combination of two distinct thermal process steps. The first is a bubbling fluidised bed gasifier operated at 700-800 ˚C in which steam and oxygen are used to partially oxidise the waste derived fuel. In the second step, the crude syngas produced by the bubbling bed gasifier is exposed to extreme conditions (T ~ 1200 ˚C) in a separate plasma converter(Materazzi et al. 2016). The plasma converter completely degrades complex hydrocarbons and tars reducing them to a clean syngas stream along with simple inorganic contaminants such as hydrogen sulphide and hydrogen chloride which are readily removed with conventional gas scrubbing techniques. The choice of a two-stage process was to ensure the production of a consistent quantity of syngas form a chemically and

physically heterogeneous feedstock, of a quality suitable for chemical transformation as opposed to energy production. With this respect, the reforming action of electric plasma not only ensures stable operation and higher carbon conversion efficiency (due to the conversion of tars and fly char into more H_2 and CO), but also simplifies the pool of contaminants that need to be removed downstream. In fact the plasma breaks down covalently bound organic sulphur (e.g. thiophenes, thioles, and their derivatives) and other problematic contaminants, and transforms them to mostly H_2S. Thiophene in particular, although rarely measured in small scale plants, has been found to be particularly detrimental in catalytic systems, even at below ppm levels, due to the high sensitivity of synthesis catalysts to sulphur in all its forms (Rabou & Bos 2012; Rhyner et al. 2014). This is hardly removed by conventional scrubbers (Kaufman Rechulski et al. 2014) and reported to be one of the main obstacles in the use of waste fuels for BioSNG production (Czekaj et al. 2007).

Downstream of the plasma arc converter, the syngas is cooled to below 200 °C in a heat exchanger prior to treatment to remove any residual particulates and elementary acid gas contaminants (mostly, HCl, COS, and H_2S). This includes a dry filter (incorporating a ceramic filter unit with sodium bicarbonate and activated carbon dosing), an alumina hydrolysis reactor to convert any residual COS to H_2S, and then an oxidative alkaline wet scrubber. This provides bulk removal of nitrogenous compounds, chloride, fluoride, and simple sulphur gases present prior to demisting to reduce entrained water. An iron oxide pellet guard bed is used for any residual sulphur scavenging. Slightly negative pressure (5–10 mbar) is maintained using an induced draft (ID) fan located after the wet scrubber.

2.2.2. Gas storage and Syngas supply

The outlet of the ID fan defines the system boundary between the original 500 kW_{th}

gasification pilot facility and the new BioSNG plant. In order to separate the operation of the two plants, the syngas from the gasification process is compressed and stored. The syngas is generated at approximately 0.05 barg pressure and is compressed to 50 barg through a four-stage reciprocating compressor, featuring interstage cooling with condensate removal. The compressed syngas is then supplied to the BioSNG gas store, which comprises four identical gas storage vessels. These vessels are capable of holding approximately 1.2 tonnes of compressed syngas, whose composition is reported in Table 3. Each vessel features inert gas purge, pressure relief and vent connections.

Table 3 Syngas specification used for baseline tests

Quality Parameter:		**Stored syngas**
Composition:		
H_2	vol.%	35.77
CO	vol.%	33.20
CO_2	vol.%	23.54
CH_4	vol.%	1.67
H_2O	vol.%	0.89
Other	vol.%	4.90
TOTAL	vol.%	100.00
Trace contaminants		
H_2S + COS	ppmv	< 50
Organic sulphur	ppbv	< 30
Tars (+C6)	µg/m^3	< 18
Acetylene	ppmv	< 40
Tot. Chlorine	ppmv	< 10
Energy Analysis		
Net Calorific Value	MJ/kg	8.75

When the second part of the plant is in operation for BioSNG production, this receives syngas from the high pressure store and a heater electrically heats the syngas before releasing the pressure to the required plant operating pressure (in the range 1 to 20 barg). This initial heating is required to prevent the formation of solid, frozen carbon dioxide in the process pipework due to excess cooling during pressure reduction.

2.2.3. Water Gas Shift Reaction

The syngas is then electrically heated by further heaters to 400°C and controlled flows of deionised water are added, which is then vaporised to form steam. The steam-laden syngas is then electrically-heated to provide the feed gas to the water gas shift reactor. The High-Temperature Water Gas Shift Reactor (WGS) comprises a tubular reaction vessel containing a suspended canister containing commercial ferro-chrome catalyst beads. In this reactor the syngas components are combined to enhance the hydrogen content via the water gas shift reaction:

$$H_2O\ (g) + CO\ (g) \leftrightarrow H_2\ (g) + CO_2\ (g)$$

Water gas shift reaction is a moderately exothermic reversible reaction yielding 41.09 kJ/mol. Residual COS in the gas would also be hydrolysed to produce H_2S. The shifted syngas from the High Temperature Water Gas Shift Reactor passes through a single Guard Bed tubular reactor (GB-1) containing a suspended canister of zinc oxide in which any residual sulphur contaminants (principally hydrogen sulphide) within the gas are removed. Some or all of the cleaned, shifted syngas from the Guard Bed passes through a water-cooled heat exchanger (HX-1) so as cool the gas to a temperature appropriate for that required for downstream methanation reactors.

2.2.4. Methanation Reactors

The cooled shifted syngas is then fed to the methanation reactors. The gas can be sent to any or all of the three physically-identical methanation reactors. The reactors (MTH-1, MTH-2, and MTH-3) are physically identical and contain a suspended canister containing differing catalyst beads, comprising commercially available nickel-based catalysts of increasing activity. 8%Ni-Al_2O_3 and 12%Ni-Al_2O_3 (Catal International) were successfully used as the bulk catalysts in the first two reactors MTH-1 and MTH-2, respectively. The catalysed reaction in both vessels lights off at

approximately 330°C. A higher activity 22% Ni-Ca-Al_2O_3 was used in MTH-3, where very high CO conversion and methane selectivity are required. As the gas passes through these catalyst beds the hydrogen and carbon monoxide within the shifted syngas are reacted together to produce methane, thus:

$$3H_2\ (g) + CO\ (g) \leftrightarrow CH_4\ (g) + H_2O\ (g)$$

This reaction is highly exothermic producing 206 kJ/mol and leads to significant rises in temperature across the reactors. To control and mitigate this temperature rise, which reduces methane yield, the methanation reaction chain incorporates a number of features including inter-reactor cooling through a water-cooled heat exchanger unit; individual control of addition of inert diluent gas to each of the methanation reactors, individual control of fresh shifted syngas feed flows to each methanation reactor, the ability to divert some or all of the product gas flow from the individual methanation reactors so bypassing downstream reaction stages, and an ability to cool the shifted syngas feed flows (Kopyscinski et al. 2010). As the shift syngas passes through the series of methanation reactors the concentration of methane rises steadily up to approximately 30-40% (dry basis) - depending on the composition of the syngas and/or waste treated - while the levels of hydrogen and carbon monoxide drop away to near zero levels.

2.2.5. Product Gas Conditioning

From the final methanation reactor (MTH-3) the methanation product gas is cooled through a water-cooled heat exchange unit (HX-4) and thence to a knock-out pot (KOP) where any condensed water droplet are separated and removed from the gas stream. This gas mixture is then passed to a pressure swing absorption (PSA) unit where the gases are separated from one another to yield a methane-rich product stream and a carbon dioxide-rich tail gas stream. The plant has been specifically

designed to operate over a broad range of conditions, with flows of up to 100 kW (of thermo-chemical energy) of inlet gas, and at reaction pressures of between 1 and 20 barg.

The gas composition is continuously monitored using an IR Xentra 4210 analyser in the gasification facility, a Gasmet Fourier Transform Infrared (FTIR) Continuous Emissions Measuring System (CEMS) and Gas Data Click! gas analyser in the BioSNG facility, and in the PSA unit a Siemens Ultramat 23 for CO/CO_2 and a Siemens Calormat for Hydrogen.

3. THEORETICAL BASIS

3.1 Model development

The design and operation of the BioSNG process requires understanding of the influence of syngas and operating parameters on the performance of the plant. Especially for a multiple stage process, modelling results can provide guidance on the optimization of the process parameters, so that one can find the best operation condition between the different parts.

The gasification and methanation processes have been modelled using the Aspen Plus software. The proprietary model involves disaggregating the process into individual unit operations and then applying appropriate Aspen Plus building blocks to mimic the operation. These building blocks are then linked to provide an overall process model. The different stages considered in Aspen Plus simulation, in order to show the BioSNG process, are water gas shift (WGS), guard bed for trace sulphur polishing, three stage methanation with intercooling, condensate removal and PSA separation. Figure 2 shows the flowsheet of the simplified BioSNG process model and Table 4 reports a short description of the main blocks used to model the system.

Model of the gasification plant is shown elsewhere (Ray et al. 2012) and not presented in this paper.

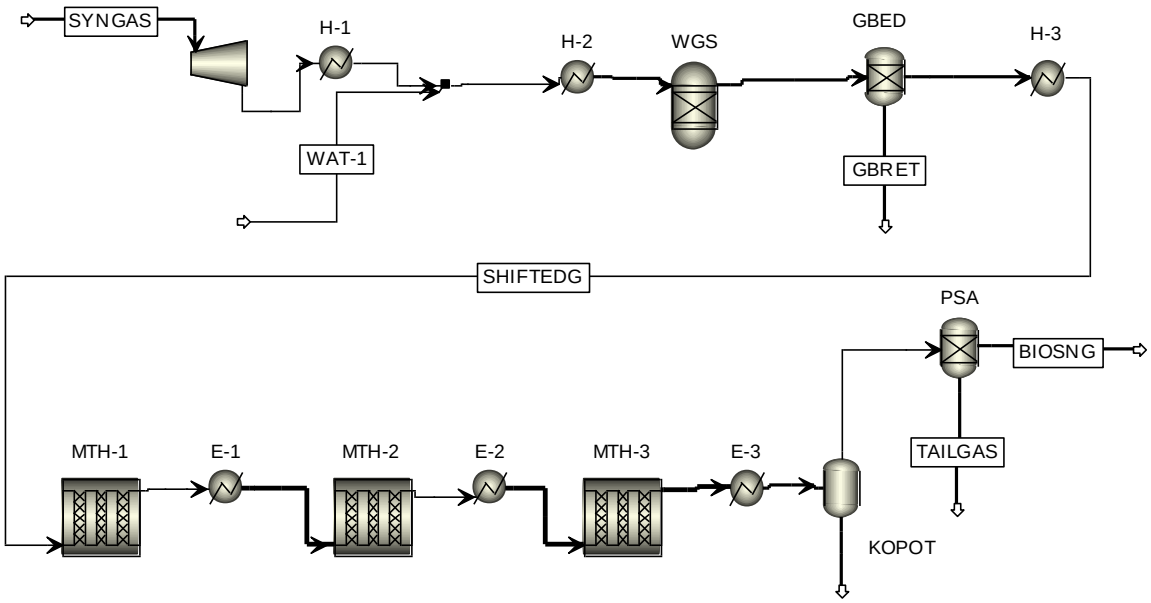

Figure 2: Simplified Aspen flowsheet for the BioSNG frontend simulation. SYNGAS: syngas from storage vessels, H-1,2,3: gas heaters, WGS: high temperature water gas shift bed, GBED: guard bed for sulphur polishing, MTH-1,2,3: methanation fixed bed, E-1,2.3: interstage coolers, KOPOT: knock-out pot vessel, PSA: Pressure Swing Adsorbtion unit, TAILGAS: CO_2 rich-stream, BIOSNG: CH_4 rich-product

Table 4 – Description of the blocks used in the Aspen simulation

Block name	Block type	Operating conditions (baseline case – Thermal load: 17-52 kW_{th})		
		Pressure (barg)	Thermal mode	Other
WGS	RGIBBS	1-20	Isothermal	Steam/gas = 1.15 Approach delT=15˚C
H-1, H-2, H-3, E-1, E-2, E-3	HEATER	No pressure drops	300, 350, 350, 50 ˚C (Outlet)	LMTD corr. factor=1
GBED	SEP	Ergun applies	PFR heat flux: 2-5 kW/m^2	Full separation
MTH-1, MTH-2, MTH-3	RPLUG	Ergun applies	PFR heat flux: 2-5 kW/m^2	Kinetic rate: LHSW Effectiveness factor = 0.01
KOPOT	FLASH	No pressure drops	Isothermal	Calculate V/F and Heat
PSA	SEP	-	Isothermal	Separation data from supplier

Stored syngas composition is specified in the SYNGAS stream according to Table 3, along with flowrate and thermodynamic conditions. The Aspen Plus Gibbs reactor, RGIBBS, was used to simulate the water gas shift. In this block, the H_2/CO ratio is adjusted to the desired value by injecting limited amount of de-ionised water (WAT-1), and outlet composition is determined by specifying the reactor temperature according to thermodynamic equilibrium. Residual COS in the gas is also hydrolysed in WGS with produced H_2S being sequestered in the guard bed (GBED). Upon being heated to 350 °C, the shifted syngas (SHIFTEDG) is reacted in 3 sequential methanation steps (MTH-1, MTH-2, MTH-3), each modelled by the RPlug reactor in Aspen. The development of the methanation section has been informed by a combination of published data and the operation of lab experiments to account for the kinetic equations and resultant compositions which cannot be calculated from thermodynamic equilibria. In the present work, a Langmuir–Hinshelwood type model was employed for simulation of the reaction rates at different thermodynamic conditions (Table 5). Reaction modelled in the Rplug reactors include both CO methanation and water gas shift reactions, adapted from the literature (Xu & Froment 1989). Experiments were conducted in a laboratory catalytic test facility to calculate the kinetic parameters for the examined catalyst (Materazzi et al. 2017). In particular the pre-exponential factors (k_i^0) and energies of activation factors (E_i) were adjusted to fit experimental data.

Table 5 – Kinetic models for water gas shift and methanation reactions implemented in Aspen RPlug units (adapted from Xu & Froment 1989)

	Model parameters:		Units:
$r_{MTH} = \frac{k_{MTH}}{P_{H2}^{2.5}}\left(\frac{P_{CO}P_{H2}^{3}}{K_{MTH}} - P_{CH4}P_{H2O}\right)/DEN^{2}$	k_{MTH}^{0}	9.89 x 10^{16}	(mol $bar^{0.5}$)/(g h)
	E_{MTH}	248	kJ/mol
	k_{WGS}^{0}	5.23 x 10^{6}	(mol $bar^{0.5}$)/(g h)
	E_{WGS}	57.9	kJ/mol
$r_{WGS} = \frac{k_{WGS}}{P_{H2}}\left(P_{CO}P_{H2O} - \frac{P_{CO2}P_{H2}}{K_{WGS}}\right)/DEN^{2}$	K_{CO}^{0}	8.23 x 10^{-5}	Bar
	ΔH_{CO}	-70.65	kJ/mol
	K_{H2}^{0}	6.12 x 10^{-9}	bar
	ΔH_{H2}	-82.90	kJ/mol
$DEN = 1 + K_{CO}P_{CO} + K_{H2}P_{H2} + K_{CH4}P_{CH4} + K_{H2O}P_{H2O}/P_{H2}$	K_{CH4}^{0}	6.65 x 10^{-4}	bar
	ΔH_{CH4}	-32.28	kJ/mol
$k_i = k_i^{0}\exp\left(\frac{-E_i}{RT}\right)$ $\quad i = MTH, WGS$	K_{H2O}^{0}	1.77 x 10^{5}	bar
$K_i = K_i^{0}\exp\left(\frac{-\Delta H}{RT}\right)$ $\quad i = H_2, CO, CH_4, H_2O$	ΔH_{H2O}	88.68	kJ/mol

Preliminary experiments using the same catalyst on CO_2-free and CO_2-rich gas mixtures have shown the CO conversion was similar in the two cases, suggesting that CO_2 does not affect significantly the methanation reaction, at least at the conditions explored in this work (Materazzi et al. 2017). This is in line with other studies which report that CO_2 methanation is inhibited in the presence of CO and thus often not accounted in kinetic modelling (van Herwijnen et al. 1973). Furthermore, the deactivation modeling was beyond the scope of the present paper. The model is automatically adjusted to provide reactor temperatures and space gas velocity (GHSV) conditions in the reactors that match those observed for the pilot plant.

For the purposes of this assessment, the PSA unit was modelled as a simple component separator based on separation curves provided by the unit supplier. For the thermodynamic model, the RKSMHV2 is used. The RKSMHV2 property method is based on the Redlich – Kwong - Soave equation of state with modified Huron-Vidal mixing rules (Michelsen 1990). This model is used for mixtures of non-polar and polar compounds, in combination with light gases. All the binary interaction parameter values needed for these models were provided by Aspen library.

The model, based on real information derived from operation of the pilot plant, could also be used to determine the performance of plants at larger scale. The scaling of the main reactors for example (i.e. water gas shift and methanation) is based on the following separate parameters:

- **Thermal load**. This parameter is defined as the syngas energy content per unit weight of catalyst and is used to define the bed configuration. The pilot plant trials and syngas composition are used to define this thermal loading for models.
- **Operating temperature**. Trials provide evidence of the acceptable temperatures at which the exothermic reactions can be performed to achieve both the desired gas quality and avoid sintering and thermal degradation of catalysts. For this study, a maximum temperature of 500 °C in the catalytic beds has been set (based on catalyst supplier indication).
- **Operating Pressure**. The system can run at any pressure from 1 to 20 barg. Kinetic models have been selected to take into account the pressure influence.
- **Space gas velocity**. Syngas and steam are used as the only reactants within the reactors which are not equipped with product recycle loops. The flow of

these agents is a function of the desired operating temperature and residence time within the reactor.

- **Heat losses**. System heat losses must be overcome by heat generated by exothermic reactions. Models of these heat losses have been developed for the pilot plant and are confirmed by equipment skin temperature measurements. These same equipment skin temperatures are then imposed on Aspen models to provide assessments of the heat losses to be experienced at different scales.

The preliminary results from the plant operation after start-up and catalysts activation were used to validate the model. The inlet conditions and operating parameters for the base case are tabulated in Table 6.

Table 6 50 kWth pilot plant parameters for model validation

Description:	
Reactor(s) diameter (m)	0.12
Reactor(s) height (m)	1.3
Methanation catalysts (MTH-1,2 / 3)	
Nickel content (wt. %)	8-12 / 22
Reduction temperature (ºC)	400
Particle size (mm)	2.8-3.4
Thermal conductivity of catalyst (W/m K)	0.2
Particle density (g/cm^3)	3.9
Dilution factor (wt. inert / wt. catalyst)	0-0.5 / 0
Operating conditions:	
Inlet pressure (barg)	1-12
Steam inlet temperature (ºC)	250
Syngas molar flowrate (kmol/h)	0.24-0.8

4. RESULTS AND DISCUSSION

4.1. Model validation

To determine whether the Aspen simulation of the BioSNG plant predicted

reasonable product compositions, 3 simulated key product streams (WGS, first methanation and PSA outputs) were compared with those obtained by the pilot plant for a baseline case. The intermediate product compositions for the Aspen simulation and the pilot design are shown in Table 7;

Table 7: Gas composition at 3 different sampling points from the model and pilot plant

		SHIFTEDG		MTH-1 Output		BIOSNG	
Quality Parameter		Model	Pilot plant	Model	Pilot plant	Model	Pilot plant
Composition:							
H_2	vol.%	41.79	(41.65)	23.53	(21.1) #	5.45	13.57
CO	vol.%	16.57	14.96	14.18	12.82	0.02	0.17
CO_2	vol.%	31.47	31.31	31.35	29.8	1.29.	0.16
CH_4	vol.%	1.09	3.10	9.98	11.1	81.65	70.75
H_2O	vol.%	4.96	4.79	16.3	19.5	3.19	2.10
N_2 (from syngas)	vol.%	4.12	(4.15)	4.66	(5.68) #	8.45	13.25
TOTAL	vol.%	100.00	100.00	100.00	100.00	100.00	100.00
Energy Analysis							
NCV	MJ/kg	7.77		7.34		38.04	

calculated

Values have been averaged over approximately 60 hours of continuous operation, which was the maximum allowed by the four gas storage vessels at the examined gas throughput. The downstream gas processing and polishing techniques have been shown to provide syngas of sufficient quality for catalyst operation, with no evidence of sulphur induced degradation, nor other contamination or deactivation during the run.

Although the Aspen simulation of the methanation unit predicts slightly lower conversion of carbon monoxide and carbon dioxide than pilot plant's, the conversions agree to within 5-10%. During steady state operation, methane was produced at rates between 12 and 26kWth and at concentrations of 9-12% in volume, equating to 30-33% CO conversion in the first reactor only. This is slightly lower than the equilibrium value of conversion but compares favourably with the 31% predicted by the process model, as shown in Table 7. This better performance may

be due to higher system thermal losses that permit the reaction to be carried out at lower than adiabatic temperature increases predicted by the model. When compared to larger scale plants, the pilot plant possesses a much higher surface area relative to the amount of gas processed. Indeed, it is estimated that the relative heat losses the pilot plant used in this work are 3-10 times higher than what envisaged in a commercial plant. Although this might sound advantageous from a methane yield perspective, the thermal efficiency of plants and potential of heat recovery at such small scale would be negatively affected.

The largest discrepancy with the model was found with the PSA. The removal efficiency for CO_2 was extremely high (over 99%). This was one of the primary functions of the PSA and was achieved very effectively, even beyond expectations from the unit specifics which were set in Aspen. The other primary target components for removal were N_2 and H_2, whose projections were significantly lower. These were reduced by 40%(+/-0.15%) and 35%(+/-0.2%) respectively, although the gas safety management regulation (GSMR) would require even lower concentrations in the final BioSNG stream (Dodds & McDowall 2013). In particular, the UK currently only permits 0.1% vol. hydrogen in the network. Notwithstanding the limitations of the pilot plant, the separation performance was deemed satisfactory at this stage of development, as the plant was clearly not optimised for full H_2 and CO conversion, and N_2 entrainment level at the gasification stage can be largely contained. Pilot plant operation has also shown that in achieving higher levels of component removal, an appreciable level of methane slip could be experienced (up to 20% in the CO_2 rich stream), as a direct consequence of optimisation for removal of the non-CO_2 components. Clearly such levels of slip would not be acceptable in a

commercial plant, both from environmental or economic reasons. As stated before, the upstream process must be controlled to avoid these components from the onset, which was demonstrated to be achievable by reducing N_2 inlet through the fuel injection system, and by pushing methanation to full conversion with use of more active catalyst in the final stages (Materazzi et al. 2017).

This work may also suggest the attractive possibility of methane purification using a single unit to selectively remove CO_2 (e.g. amine scrubbers, etc.), thus maximising methane recovery and improving the overall efficiency of the process (Rao & Rubin 2002).The use of biogenic sourced CO_2 as feedstock, sometimes referred to as carbon capture and utilisation (CCU), is attracting a growing interest around the world since it can increase conversion efficiency and reduce dramatically CO_2 emissions (Quadrelli et al., 2015). For example, CO_2 can be transformed into various bulk chemicals (including more BioSNG), utilising hydrogen produced via renewable sources, i.e wind or solar, when a surplus of electricity is available. With this respect, one application that is attracting much attention is Power-to-Gas (Götz et al., 2016). This technology involves the production of hydrogen from (variable) electricity via dynamic operation of an electrolyser. Since hydrogen is difficult to store and distribute, methane is generally the preferred gaseous product. In this case, it can also be noted that a derogation to introduce gas with higher levels Hydrogen, as allowed elsewhere in Europe, would simplify the plant, lowering capital and operational costs (Messaoudani et al. 2016). In Germany for example, up to a 10% vol. of Hydrogen in natural gas is permitted, and a few projects have already undertaken hydrogen injection to the national gas grid (Ogden et al. 2018).

4.2. Adiabatic vs Isothermal Operation

A reactor operates adiabatically when no heat is gained or lost by the system. For an exothermic reaction, such as WGS and methanation, carried out adiabatically, temperature increases with reaction progress. When a reaction is highly exothermic, as in MTH-1 and MTH-2, a temperature increase can generate a thermal runaway and catalyst deactivation. To overcome this problem, several methods are used such as: isothermal reactor, adiabatic reactor with recycling, fluidized bed reactor and addition of steam (Rönsch & Kaltschmitt 2012).

The benefits of an adiabatic reactor are the relatively simple equipment construction and the maintenance, which are very important if small devices are being designed. In reality, a portion of thermal energy is always lost as dissipated heat through the reactor walls and pipes, and the term '*quasi-adiabatic*' would be more appropriate to describe such systems. In the present work, quasi-adiabatic multistage methanation reactors with intermediate cooling have been modelled. The substantial difference from other multistage adiabatic fixed beds (as in TREMP, for example) is the absence of a recycling stream to control the temperature and the equilibrium conversion. CO_2 and steam are retained in the gas for this purpose, and intermediate cooling is used to displace the gas temperature in the direction of higher equilibrium conversion. This temperature should be below the highest temperature allowed by the catalyst manufacturer and greater than catalyst activation one, also known as *'light-off'* (or ignition) temperature. In the case of exothermic methanation reaction, CO conversion decreases with increasing temperature. Equilibrium curve which represents CO conversion as a function of the gas temperature is calculated by using minimization of Gibbs energy method in Aspen, and shown in Figure 3 (dashed line). The calculation of the diagonal lines is

based on the energy balance of each MTH unit, as modelled in Aspen. In each reactor the methanation reaction will take place pointing towards thermodynamic equilibrium direction. The variation of the CO conversion with respect to thermodynamic equilibrium can be illustrated for the three methanation reactors by joining diagonal lines for the quasi-adiabatic reaction (MTH-1, MTH-2, MTH-3) to horizontal lines for the temperature reduction due to intermediate cooling (E1, E2).

The initial CH_4 flow is 16.7 mol/h (total flow of wet feed gas is ~540 mol/h) and the inlet temperature and pressure of the first two methanation reactors MTH-1 and MTH-2 are 350°C and 6 barg, respectively. This temperature has been set on the basis of the light-off conditions (~340 ˚C, 1 barg) of the low-Ni catalysts contained in the first two reactors. Here the total amount of CO converted is approximately 60%, which is accompanied by a temperature increase of 160°C for each reactor (outlet temperature is ~500°C). Allowing the reaction to proceed further would increase the risk of carbon deposition and catalyst deactivation. The cooler E2 cools the gas to 250°C, i.e. the inlet temperatures of the reactors MTH-3, which contains the more active catalyst. After the third reactor the CH_4 flow is 87.1 mol/h, which corresponds to a combined CO conversion of 95.3%. By comparing heat losses with temperature rise, the exotherm in the first two reactors was assessed to be around 180 kJ/mol, i.e. lower than reported figures for CO methanation (206 kJ/mol) and higher than that for CO_2 methanation (165 kJ/mol). This is further confirmation that the reaction set is more complex than simple CO-methanation, and suggests that more work is needed in this direction (Panagiotopoulou et al. 2009).

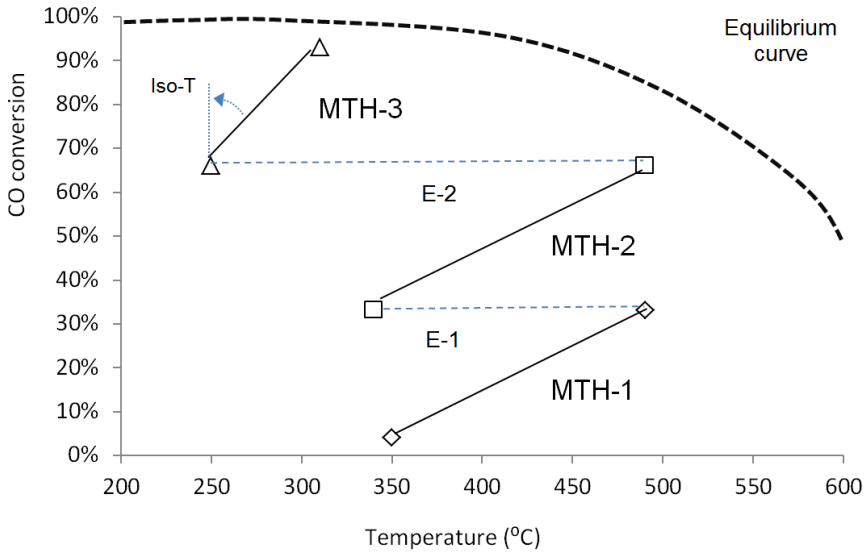

Figure 3: Variation of CO conversion and reactor temperature in the methanation system operated at 6 barg. Feed flow is 540 mol/h with 16.7 mol/h of initial CH_4

Incidentally, a lower temperature increase is observed in the last reactor, mainly due to the lower content of CO to be converted and higher quantities of product methane and steam from previous stages that act as thermal diluents. As a result, the heat generated by exothermic reactions is only slightly higher than the system heat losses, with the system approaching a more isothermal-type operation. This, along with the presence of a catalyst active at a lower temperature, allows greater conversion to be achieved, with values above 95% at a relatively low pressure. Higher conversions could be achieved through different routes, e.g. by increasing pressure (see Section 4.3.4), or controlling the reaction at fully isothermal conditions by using a different catalyst and/or reactor configuration. Fluidized bed reactors, for example, have demonstrated to be an attractive alternative because they provide good catalyst mixing and the high heat transfer rates needed to maintain isothermal operation (Seemann et al. 2006). Thus, undesirable hot spots with strong tendencies towards carbon deposition are avoided.

4.3. Parametric study

The purpose of the parametric study was to determine the effect of operating conditions on product composition, thermal efficiency of the process, and outlet temperature from methanation reactors. The operating conditions that were varied on the model were: the ratio of steam added to the shift reactor to the total syngas unit feed, the H_2/CO ratio in the feed syngas, the feed temperature in the methanation reactor(s), and gas space velocity. When available, pilot plant data are added for direct comparison.

4.3.1. Steam-to-Feed Ratio

Steam provides a number of important functions in system control. According to Le Chatelier's principle, it is expected that an increase in steam will enhance water gas shift reaction and inhibit methanation reactions.

As discussed in Section 2.2.3, process steam is added as controlled flows of either steam, or steam-forming deionised water before the water gas shift reactor. The excess steam that does not react in the WGS unit, is carried along with the gas directly into the methanation section. Here, steam has the important function to prevent carbon deposition and to absorb sensible heat so a higher conversion of carbon monoxide and carbon dioxide to methane can be obtained for a given temperature rise in the reactor.

The effect of the steam-to-feed ratio on process thermal efficiency, outlet temperature of the first reactor, conversion in the first reactor, and percentage hydrogen and carbon monoxide in the product was determined for Steam-to-Carbon

(S/C) molar ratios of 0.01 to 0.65. This is defined as the ratio between the added steam and the total carbon present in the gas as CO, CO_2 and CH_4. The base-case conditions given in Table 4 were used for all other process conditions and the main results are shown in Figure 4.

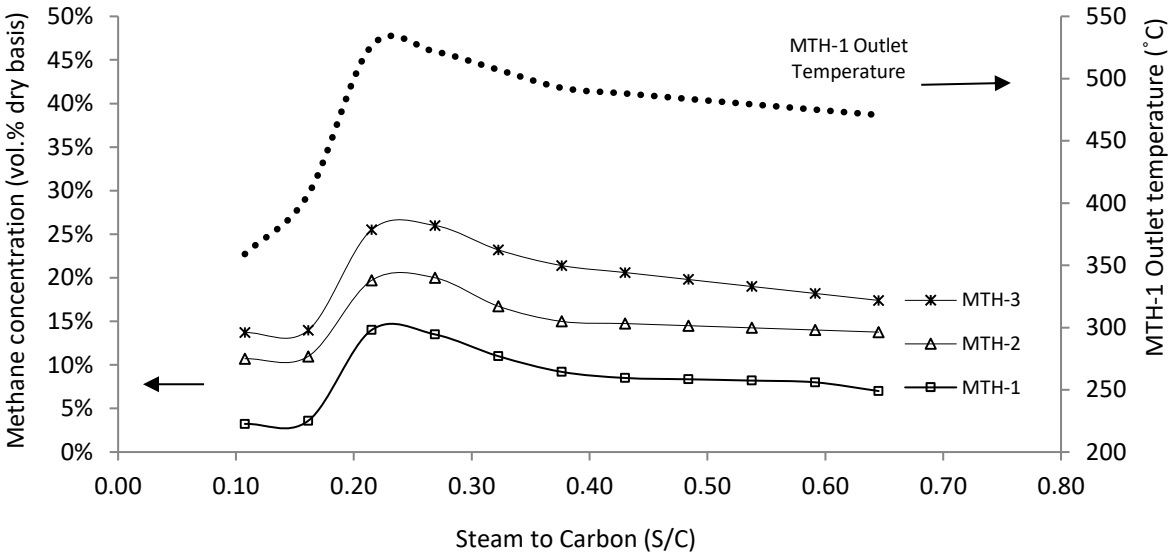

Figure 5: Variation of methane concentration and reactor temperature in the methanation system at different steam to carbon (S/C) ratios (model results).

At low S/C ratio, the plant is unable to deliver the required H_2:CO ratio of 3:1. As a consequence, whilst CH_4 levels of around 14% could still be achieved, levels of H_2 and CO at the exit of the third reactor would be too high to comply with the specifics of the PSA.

At S/C ratio equal to 0.2, a higher H_2:CO ratio downstream the WGS unit is obtained, and higher stoichiometric conversion in the first MTH reactor is possible. Higher levels of steam addition also result in higher levels of CO_2 in the outlet stream, highlighting the influence of the water gas shift reaction in the system. Higher methane production, especially in the first reactor, is also due to the fact that the additional steam absorbs some of the heat of reaction; therefore, more carbon

monoxide and carbon dioxide react for the same temperature rise across the reactor. Accordingly, less carbon monoxide and carbon dioxide react in the second reactor, which could also operate at lower temperature.

Figure 4 also shows that the temperature of the outlet stream from the first reactor was higher than the catalyst could tolerate in the case where the 0.2 S/C ratio was used, so higher ratios are needed. The product temperature and the methane concentration slightly decrease when more steam was added (S/C > 0.4) because the additional steam changes the equilibrium conversion. The hydrogen product specification (< 5 mole % hydrogen before PSA) was not met in the cases tested; however, when the higher (> 0.2) S/C ratio was used, the carbon monoxide was always lower than 0.5%. This suggests that a further catalytic stage for combined CO_2 and CO hydrogenation could be attempted in the future.

The disadvantage of adding more steam is that more residual H_2 is produced within the process and less energy could be recovered through gas cooling. Because high steam-to-feed ratios result in lower thermal efficiencies in a commercial plant, the other parametric studies used an intermediate ratio (0.25) to determine whether product specifications and operating constraints could be met by varying other operating conditions.

From a purely operational point of view, steam was also found to have an important role in controlling carbon deposition. This is important as it could not only cause deactivation of the catalyst by encapsulation, but may even result in destruction of the catalyst and blocking of the reactor because of excessive growth of filamentous carbon within the pores (Bartholomew 2001). Additional trials on the pilot plant demonstrated that inconsistency or absence of steam led to significant

carbon deposition. However this could be effectively controlled by steam addition.

4.3.2. Syngas composition

The average conversion efficiency of CO for the first methanation unit (MTH-1) at baseline case was approximately 33%. Conversion efficiency and selectivity towards methane were found to be strongly dependent on H_2:CO ratio at the methanation inlet, as also shown in previous section; at H_2:CO of 4:1, conversion was around 35%, with a 70% selectivity towards methane, whereas at H_2:CO of 2.5:1, CO conversion dropped to 28%, with a 60% selectivity towards methane. The conversion efficiency for the second methanation unit MTH-2 was found to be similarly sensitive to H_2:CO, in this case dropping from 55% to 42% with H_2:CO dropping from 4:1 to 3.5:1 respectively. At lower H_2:CO ratios, water produced by the methanation reaction reacts with CO in a shift reaction, producing CO_2. However, when there is a large excess of H_2 (>3), the reverse water gas shift reaction is favoured, and so rather than CO reacting to produce more CO_2, CO_2 produces CO which can then be methanated. As a result, selectivity to methane and overall yield improve.

The model demonstrated a moderate sensitivity to the H_2:CO ratio in the feed syngas too with both conversion and selectivity towards methane substantially reduced with a lower H_2:CO ratio (see Figure 5). This can be largely offset by adding more steam at the WGS inlet, as observed in previous section, or by enhancing the H_2:CO ratio in the syngas. Interestingly, the role of the plasma to maximize the H_2:CO ratio in the syngas is crucial to reduce the amount of steam to be fed to the WGS reactor, thus enhancing the overall efficiency of the process.

This confirms that the not-optimized H_2:CO ratio in the stored syngas is a key cause of the residual CO and/or H_2 levels, but provides confidence that under optimal conditions design levels of conversion and GSMR standards could be achieved.

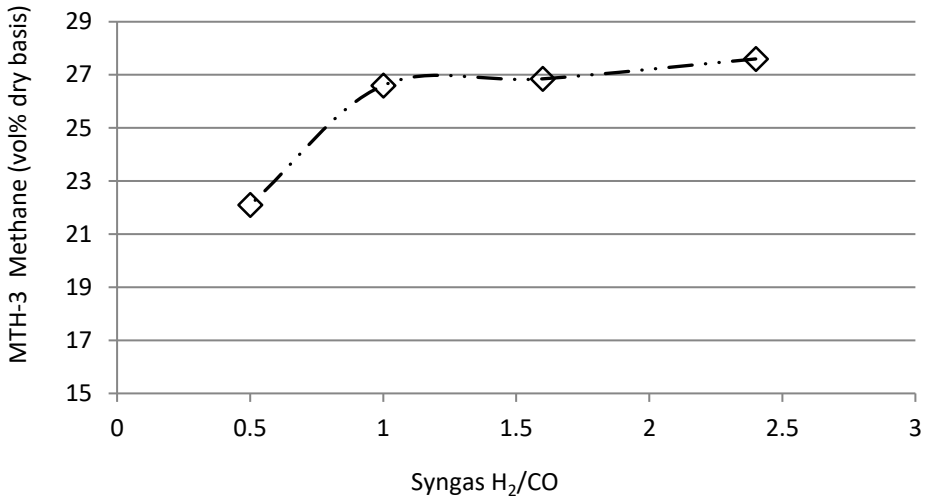

Figure 5: Variation of methane concentration from methanation system at different syngas H_2:CO ratios (model results)

The presence of CO_2 was also found to play a role in reducing overall system temperature and better controlling the process. An increase in quantities CO_2 in the product gas proved the occurrence of reverse water gas shift, which is thermodynamically favoured at high temperatures (> 400°C). Maintaining CO_2 in the gas stream through the methanation process has, therefore, a role in maintaining operational control by moderately reducing adiabatic temperature.

It was also confirmed that N_2, even at high levels did not significantly assist in exothermic control. In another work, N_2 and CO_2 were directly interchanged demonstrating clearly the above findings (Materazzi et al. 2017). Given the challenges that nitrogen presents with regard to downstream separation, it is not

suitable for full scale operation in any case, and entrainment in the upstream gasification stage should be minimised.

Together this work shows that for a once-through methanation system, retention of CO_2 in the process stream through the primary methanation phase, as well as a slight excess of steam is important in maintaining process control and catalyst activity.

4.3.3. Inlet Temperature on the first Methanation reactor

During plant operation, the temperature of the feed to the first methanation reactor MTH-1 was varied from 300 to 480 ˚C, as shown in Figure 6, to determine whether product specifications and operating constraints could be met with the other process parameters set at the base-case values given in Table 4. It is clear that there is an upward trend for methane concentration, which corresponds to an increase in CO conversion as inlet temperature decreases (from 450 to 350 ˚C). The same was reflected by the model (solid line), which shows the typical steady-state behaviour of an exothermic reaction at increasing inlet temperature. Extending the discussion to the whole plant operation, lowering the feed temperature allows producing more methane out of the first reactor, reducing the stoichiometric conversion required in the following stages to reach equilibrium. This causes a chain effect, with the other reactor outlet temperatures being lower, thus producing a higher fraction of methane in the product stream. It is also important to note that, at a high feed temperature, the risk of thermal runaway with consequent damage of the catalyst is also significantly higher (Bartholomew,, 2001). On the other hand, the disadvantage of using lower feed temperature is that the residence time in the first methanation reactor has to

increase due to slower reaction kinetics. In Figure 6 it is evident that, at temperatures close to 300˚C, i.e. near the light-off temperature, the performance of methanation in the first reactor deteriorates significantly due to limitations in the reaction kinetics.

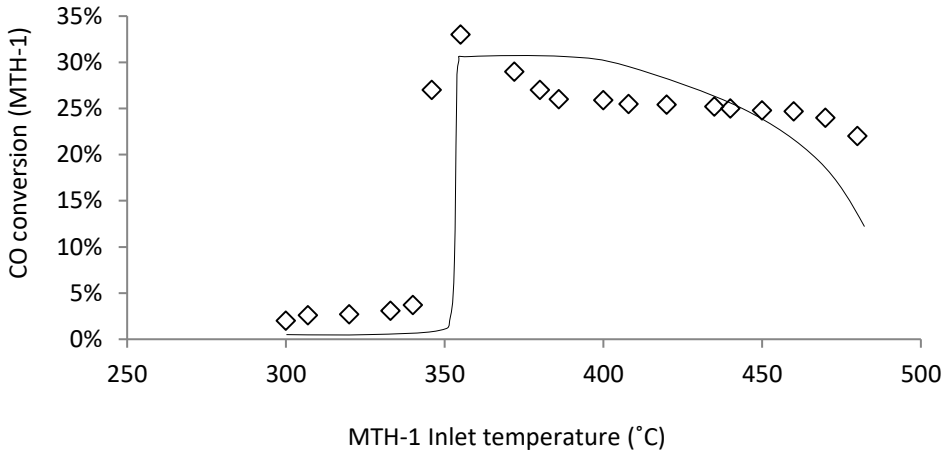

Figure 6: Variation of CO conversion in the first methanation reactor at different inlet temperature. Symbols represent experimental results gathered from pilot plant trials.

4.3.4 Operating Pressure

Apart from the discussed temperature influence, also the pressure dependence of the methanation reaction has an important function. Figure 7 visualizes the conversion of carbon monoxide at equilibrium affected by the methanation reaction as a function of temperature and pressure. Figure 7 clearly shows that the conversion of carbon monoxide increases with increasing pressure and decreasing temperature, as expected. At pressure of 1 barg and reaction temperature of 500°C for instance, a carbon monoxide conversion of 78% could be achieved. By increasing the pressure to 6 barg and keeping the temperature at 450°C, the carbon monoxide conversion reaches approximately 93%, as also demonstrated by pilot trials. Interestingly, a further increase of the operating pressure does not significantly

increase the methane yield. This could be partially due to the fact that with increasing methanation pressure, the temperature has a tendency to increase as well. On the other hand, a higher operation pressure of the fixed bed methanation technology would require a compression of a larger gas flow prior to methanation, thereby resulting in a higher power consumption and vessel material requirements. The choice of the operating pressure is, therefore, based purely on the economics of the process and final use of the product gas (Heyne at al. 2010).

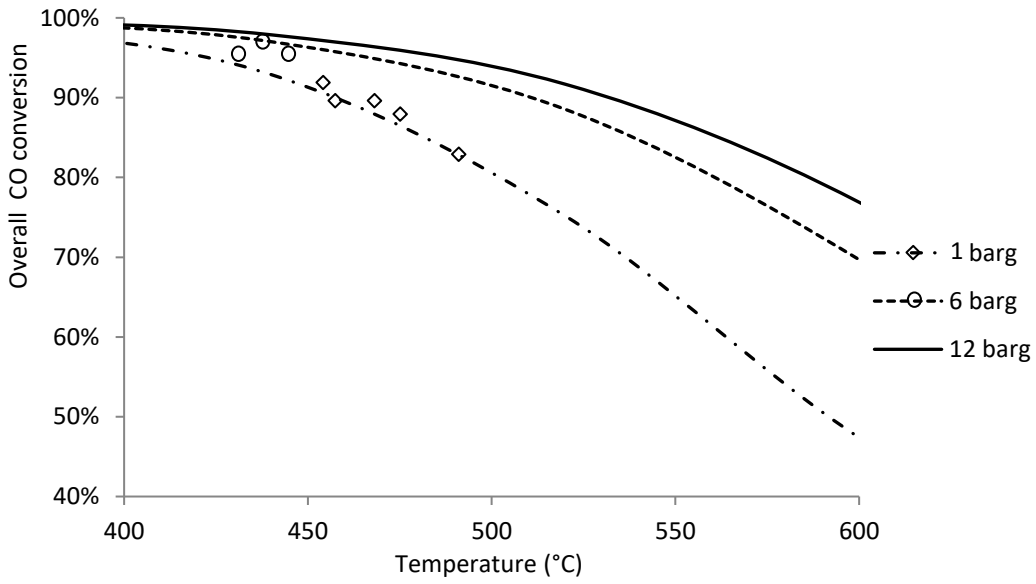

Figure 7: Variation of overall CO conversion the methanation system at different pressures. Symbols represent experimental results gathered from pilot plant trials.

4.3.6. Space velocity

A number of tests were undertaken to establish the relationship between methane production and space velocity, an example of which is shown on Figure 8. The outlet temperature was maintained below 450°C, and space velocity was varied between 0.35 and 1.5 times the baseline. The clear correlation between residence time and

conversion indicates that the catalyst conversion activity is similar across the range of space velocities. At low space velocities equilibrium is approached and further reduction gives only minimal additional methane production.

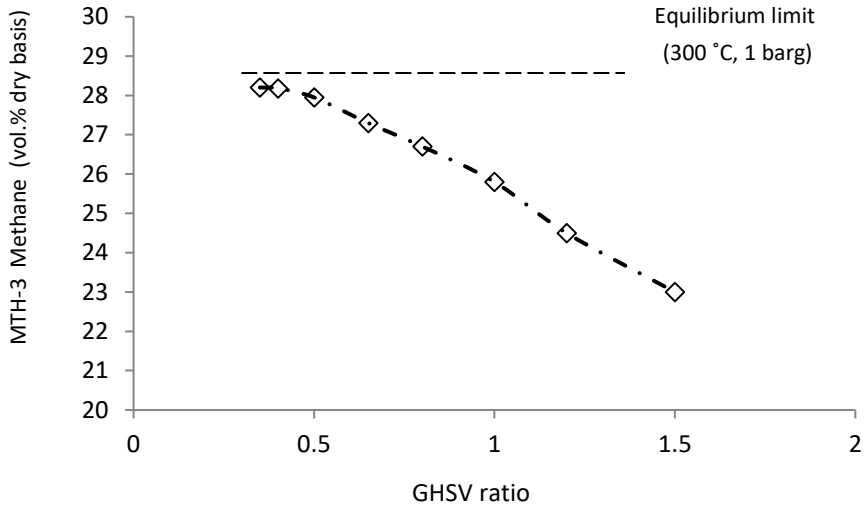

Figure 8: Methane production as Space Velocity (GHSV) is varied from baseline case (GHSV = 10,000 h^{-1})

5. CONCLUSIONS

The work presented in this paper has demonstrated that it is possible to produce methane from a waste feedstock. The combination of an oxy-steam fluidised bed gasifier directly coupled to a tar cracking plasma unit delivers a high quality raw gas with very low levels of organo-sulphur compounds. The downstream gas processing and polishing techniques have been shown to provide syngas of sufficient quality for catalyst operation, with no evidence of sulphur induced degradation, nor other contamination or deactivation for the entire duration of the experimental campaign.

The fundamentals of a once-through methanation process train have been established on the demonstration facility. For a once-through methanation process,

retention of CO_2 as well as adequate partial pressure of H_2O in the process stream is important for process control. Steam in particular is found to mitigate carbon deposition in the catalyst beds.

The high degree of correlation between model predictions and demonstration plant, gives confidence in the thermodynamic and kinetic modelling and therefore ability to predict performance on the commercial plant. This allows rapid assessments of different scale, configuration and feedstock types. Overall, there is good comparison between the model prediction and pilot plant results, with the predicted values deviating from the experimental results within the range of 5–10%. Differences are considered to be due to syngas flow uncertainties and thermal losses within the system rather than from the predictive model. This plant also provided demonstration of the efficacy of a PSA system for separation of CO_2 as well as the potential to remove a proportion of residual H_2, N_2 and CO, although this was associated with appreciable CH_4 slip. Whilst a PSA is feasible for this application, alternative separation techniques need to be considered. Furthermore, the prospect of integration with the waste heat available from the methanation process, and the production of high quality CO_2 stream which would be suitable for industrial sales or Power-to-Gas applications are deemed important for the overall efficiency of the process. Future work will focus on further observations on the integrated system, longevity tests during long term (> 2000 h) trials, and effect of waste associated gases on reactors operation.

AKNOWLEDGEMENTS

The authors wish to acknowledge the GoGreenGas consortium for the support provided through the experimental phase and pilot plant demonstration. The project

was sponsored from both Ofgem's Network Innovation Competition and the European BESTF-ERANET programme.

REFERENCES

Ardolino, F., Parrillo, F. & Arena, U., 2018. Biowaste-to-biomethane or biowaste-to-energy? An LCA study on anaerobic digestion of organic waste. *Journal of Cleaner Production*, 174, pp.462–476.

Arena, U. et al., 2015. A techno-economic evaluation of a small-scale fluidized bed gasifier for solid recovered fuel. *Fuel Processing Technology*, 131, pp.69–77.

Arena, U. & Di Gregorio, F., 2014. Energy generation by air gasification of two industrial plastic wastes ina pilot scale fluidized bed reactor. *Energy*, 68, pp.735–743.

Arvidsson, M. et al., 2012. Integration opportunities for Substitute Natural Gas (SNG) production in an industrial process plant. *Chemical Engineering Transactions*, 29, pp.331–336.

Bartholomew, C.H., 1982. Carbon Deposition in Steam Reforming and Methanation. *Catalysis Reviews*, 24(1), pp.67–112.

Bartholomew, C.H., 2001. Mechanism of catalyst deactivation. *Applied Catalysis A: General*, 212, pp.17–60.

Caputo, A.C. & Pelagagge, P.M., 2002. RDF production plants: I Design and costs. *Applied Thermal Engineering*, 22(4), pp.423–437. Available at: http://www.sciencedirect.com/science/article/pii/S1359431101001004 [Accessed September 7, 2015].

Cozens, P. & Manson-Whitton, C., 2010. *BioSNG: Feasibility Study. Establishment of a Regional Project*, Available at: http://www.biogas.org.uk.

Czekaj, I. et al., 2007. Characterization of surface processes at the Ni-based catalyst during the methanation of biomass-derived synthesis gas: X-ray photoelectron spectroscopy (XPS). *Applied Catalysis A: General*, 329, pp.68–78.

Dodds, P.E. & McDowall, W., 2013. The future of the UK gas network. *Energy Policy*, 60, pp.305–316.

E4tech, 2014. Advanced Biofuel Feedstocks – An Assessment of Sustainability. *Framework for Transport-Related Technical and Engineering Advice and Research (PPRO 04/45/12)*, 2, pp.1–82.

Gassner, M. & Maréchal, F., 2012. Thermo-economic optimisation of the polygeneration of synthetic natural gas (SNG), power and heat from

lignocellulosic biomass by gasification and methanation. *Energy & Environmental Science*, 5(2), p.5768. Available at: http://xlink.rsc.org/?DOI=c1ee02867g.

Heidenreich, S. & Foscolo, P.U., 2015. New concepts in biomass gasification. *Progress in Energy and Combustion Science*, 46, pp.72–95.

Iacovidou, E. et al., 2018. Technical properties of biomass and solid recovered fuel (SRF) co-fired with coal: Impact on multi-dimensional resource recovery value. *Waste Management*, 73, pp.535–545.

Kaufman-Rechulski, M.D., Schildhauer, T.J. & Biollaz, S.M.A., 2011. Organic sulfur compounds in the producer gas from wood and grass gasification. In *19th European Biomass Conference & Exhibition*. pp. 1625–1627.

Kopyscinski, J., Schildhauer, T.J. & Biollaz, S.M.A., 2010. Production of synthetic natural gas (SNG) from coal and dry biomass - A technology review from 1950 to 2009. *Fuel*, 89(8), pp.1763–1783.

Li, H. et al., 2015. Feasibility study on combining anaerobic digestion and biomass gasification to increase the production of biomethane. *Energy Conversion and Management*, 100, pp.212–219.

Li, S. et al., 2014. Coal to SNG: Technical progress, modeling and system optimization through exergy analysis. *Applied Energy*, 136, pp.98–109.

Mao, C. et al., 2015. Review on research achievements of biogas from anaerobic digestion. *Renewable and Sustainable Energy Reviews*, 45, pp.540–555.

Mata-Alvarez, J., Macé, S. & Llabrés, P., 2000. Anaerobic digestion of organic solid wastes. An overview of research achievements and perspectives. *Bioresource Technology*, 74(1), pp.3–16.

Materazzi, M. et al., 2017. Analysis of syngas methanation for bio-SNG production from wastes: kinetic model development and pilot scale validation. *Fuel Processing Technology*, 167, pp.292–305.

Materazzi, M. et al., 2015a. Fate and behavior of inorganic constituents of RDF in a two stage fluid bed-plasma gasification plant. *Fuel*, 150, pp.473–485. Available at: http://www.sciencedirect.com/science/article/pii/S0016236115002070 [Accessed April 2, 2015].

Materazzi, M. et al., 2016. Performance analysis of RDF gasification in a two stage fluidized bed-plasma process. *Waste Management*, 47, pp.256–266.

Materazzi, M. et al., 2015b. Reforming of tars and organic sulphur compounds in a plasma-assisted process for waste gasification. *Fuel Processing Technology*, 137, pp.259–268. Available at: http://www.sciencedirect.com/science/article/pii/S0378382015001174 [Accessed June 1, 2015].

Materazzi, M. et al., 2014. Tar evolution in a two stage fluid bed–plasma gasification process for waste valorization. *Fuel Processing Technology*, 128, pp.146–157. Available at: http://www.sciencedirect.com/science/article/pii/S037838201400280X [Accessed September 7, 2015].

Van der Meijden, C.M., Veringa, H.J. & Rabou, L.P.L.M., 2010. The production of synthetic natural gas (SNG): A comparison of three wood gasification systems for energy balance and overall efficiency. *Biomass and Bioenergy*, 34(3), pp.302–311.

Messaoudani, Z. labidine et al., 2016. Hazards, safety and knowledge gaps on hydrogen transmission via natural gas grid: A critical review. *International Journal of Hydrogen Energy*, 41(39), pp.17511–17525.

Michelsen, M.L., 1990. A modified Huron-Vidal mixing rule for cubic equations of state. *Fluid Phase Equilibria*, 60(1-2), pp.213–219.

Ofgem, 2016. *Renewables Obligation: Sustainability Criteria*, Available at: https://www.ofgem.gov.uk/system/files/docs/2016/03/ofgem_ro_sustainability_criteria_guidance_march_16.pdf.

Panagiotopoulou, P., Kondarides, D.I. & Verykios, X.E., 2009. Selective methanation of CO over supported Ru catalysts. *Applied Catalysis B: Environmental*, 88(3-4), pp.470–478.

Rabou, L.P.L.M. & Bos, L., 2012. High efficiency production of substitute natural gas from biomass. *Applied Catalysis B: Environmental*, 111-112, pp.456–460. Available at: http://dx.doi.org/10.1016/j.apcatb.2011.10.034.

Rao, A.B. & Rubin, E.S., 2002. A Technical, Economic, and Environmental Assessment of Amine-Based CO 2 Capture Technology for Power Plant Greenhouse Gas Control. *Environmental Science & Technology*, 36(20), pp.4467–4475. Available at: http://dx.doi.org/10.1021/es0158861.

Ray, R., Taylor, R. & Chapman, C., 2012. The deployment of an advanced gasification technology in the treatment of household and other waste streams. *Process Safety and Environmental Protection*, 90(3), pp.213–220. Available at: http://dx.doi.org/10.1016/j.psep.2011.06.013.

Rhyner, U. et al., 2014. Experimental study on high temperature catalytic conversion of tars and organic sulfur compounds. *International Journal of Hydrogen Energy*, 39(10), pp.4926–4937.

Rönsch, S. et al., 2016. Review on methanation - From fundamentals to current projects. *Fuel*, 166, pp.276–296.

Rönsch, S. & Kaltschmitt, M., 2012. Bio-SNG production - concepts and their assessment. *Biomass Conversion and Biorefinery*, 2(4), pp.285–296.

Seadi, T.A. et al., 2008. *Biogas Handbook*, Available at: www.lemvigbiogas.com.

Seemann, M.C. et al., 2006. The regenerative effect of catalyst fluidization under methanation conditions. *Applied Catalysis A: General*, 313(1-2), pp.14–21.

Uusitalo, V. et al., 2014. Carbon footprint of selected biomass to biogas production chains and GHG reduction potential in transportation use. *Renewable Energy*, 66, pp.90–98.

Xu, J.G. & Froment, G.F., 1989. Methane Steam Reforming, Methanation and Water-Gas Shift .1. Intrinsic Kinetics. *Aiche Journal*, 35(1), pp.88–96. Available at: <Go to ISI>://WOS:A1989R855800008.